231 (2023) 212261

Contents lists available at ScienceDirect

Geoenergy Science and Engineering

journal homepage: www.sciencedirect.com/journal/geoenergy-science-and-engineering

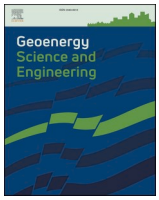

Investigation of the hydraulic integrity of cement plug: Oilwell cementitious materials

Adijat A. Ogienagbon [a,*], Mahmoud Khalifeh [a]

[a] Dept. of Energy and Petroleum Energy, Faculty of Science and Technology, University of Stavanger, Norway

A B S T R A C T

The loss of hydraulic integrity in oil and gas wells due to the loss of cement sheath sealability can lead to environmental contamination, annular pressure build-up, and safety threats. In this study, we examine the hydraulic integrity of geopolymers an alternative to cement to be used in well cementing. The hydraulic integrity of geopolymer was compared to conventional API class G and Industrial expansive cement. Down-scaled test specimens representing cement-plug in casing were prepared and tested using an in-house experimental set-up that allows continuous curing and testing of the cementitious materials under undisturbed pressure and temperature conditions. The samples were cured at 90 °C and 172 bar for 7 days after which the hydraulic sealability of the specimens was examined by applying a pressure differential to one end of the specimen and observing the resulting fluid leakage rates on the other end. The leakage rates were then expressed in terms of permeability and microannuli aperture. By injecting nitrogen and water, it was possible to compare the effects of fluid type on the hydraulic sealability of cementitious materials. Lastly, we examined the hypothesis of a linear relationship between plug length and its hydraulic sealability. The results indicate that geopolymer and Industrial expansive cement have higher hydraulic sealability compared to API class G. Geopolymers also have sufficient hydraulic bond strength to perform as much as Industrial expansive cement. The fluid type used in testing does not play a critical role in the loss of hydraulic sealability of cementitious materials. The influence of cement plug length showed varying trends on the hydraulic sealability of the cementitious materials. The results presented in this work help us understand the sealing potential of cementitious materials and the need for standards for performing laboratory-scale hydraulic sealability tests. This can benefit the improvement of cement integrity tests and well abandonment operations.

Credit author statement

Adijat A. Ogienagbon: Conceptualization, Methodology, Data Curation, Original draft preparation, Mahmoud Khalifeh: Supervision, Reviewing, and Funding acquisition.

1. Introduction

Wellbores serve as a conduit from the subsurface to the surface, they enable the extraction of energy (e.g., fossil, and geothermal) or storage of sequestrated carbon in subsurface storages. The sealability provided by wellbore cement plays a vital role in preventing interzonal migration and surface leaks of pressurized, toxic underground fluids which can cause disastrous consequences if released uncontrollably due to loss of well integrity. Therefore, well integrity must be maintained throughout the life cycle of the well. At the end of their productive life, wellbore systems need to be plugged and abandoned permanently. Plug and abandonment operations are carried out with the intention to seal the well eternally, however, this is not always the case. Plugged and abandoned wells have been identified as one of the most probable leakage contributors. In fact, cased plugged and abandoned wellbores have been reported to have a higher risk of leakage than open wells that were plugged and abandoned (Watson and Bachu, 2009). The integrity of the cement plug may be compromised at any point in the life cycle of a well. Gas migration during curing, cement shrinkage, mud channelling, thermal and mechanical stresses during well operations, and faulty cementing during plugging and abandonment are a few of the several factors that can compromise the integrity of the cement (Khalifeh and Saasen, 2020; Lavrov et al., 2015; Sasaki et al., 2018). Well leakage due to cement failure is quite common and it accounts for 33% of the leaking wells in the Gulf of Mexico (Davies et al., 2014). The casing-cement and cement-formation interfaces have been identified as preferential flow paths for the migration of fluids in a wellbore system. Fig. 1 illustrates cement leakage at the cement-casing pipe interface. It is therefore important to understand the mechanisms governing the sealability of cementitious materials at this interface.

Ordinary Portland cement has been traditionally used as a cementitious material in the industry for primary cementing and permanent plug and abandonment. However, short, and long-term complications associated with the use of Portland cement have been reported by

* Corresponding author.
E-mail address: adijat.a.ogienagbon@uis.no (A.A. Ogienagbon).

https://doi.org/10.1016/j.geoen.2023.212261
Received 14 June 2023; Received in revised form 4 August 2023; Accepted 17 August 2023
Available online 25 August 2023

Fig. 1. Leakage at the cement plug-pipe interface (Ogienagbon et al., 2021).

several researchers. The most reported shortcomings include autogenous shrinkage, low ductility, chemical instability at elevated-temperature high-pressure and corrosive environments, and loss of strength development due to mud contamination (Eid et al., 2021; Geiker and Knudsen, 1982; Sasaki et al., 2018; Shen et al., 2015). Shrinkage of the cement bulk due to the hydration reaction can increase the risk of debonding at the cement-casing and cement-formation interface causing a loss of well integrity. Over the years, researchers have proposed alternative cementitious materials like geopolymers, and expansive cement to mitigate the shortcomings associated with the use of Portland cement (Adjei et al., 2022; Khalifeh et al., 2019; Sherir et al., 2017).

A common employed technique for verifying the plug integrity of cementitious materials is hydraulic bond testing. There is a need to highlight the distinction between the shear and hydraulic bond properties of cementitious materials (Kamali et al., 2022; Opedal et al., 2018). While shear bond strength refers to the minimum force required to initiate shear failure at the interface and displace the cement sheath along the cement-casing and cement-formation interface, hydraulic bond implies the maximum force required to cause debonding and permit the leakage of fluids through the bonded interface. Hydraulic bond strength is typically determined by continuously injecting fluid at the cement-casing or cement-formation interface until tensile failure occurs and fluid breaks through (Khalifeh et al., 2018a; Ogienagbon et al., 2021). It is important to note that shear bond failure does not necessarily lead to loss of hydraulic integrity. However, a loss of hydraulic bond will permit the flow of fluids and subsequent loss of well integrity. Therefore, the hydraulic sealability of cementitious materials is more critical to zonal isolation than its shear bond properties (Bois et al., 2011).

Although several researchers have carried out hydraulic testing of various cement systems (Carter and Evans, 1964; Khalifeh et al., 2018b; Nagelhout et al., 2010; Parcevaux and Sault, 1984; Roijmans et al., 2023; Stormont et al., 2015; van Eijden et al., 2017) there is still no general consensus on a testing method. The early works of Carter and Evans (1964) extensively cover annular cement-pipe bonding. The hydraulic and gas bond between cement with steel and plastic pipes with different surface finishes were discussed in-depth. One of the numerous findings of the paper was that using gas as a test fluid typically led to a faster failure progression than when using water as a test fluid. The direction in which pressure is applied and the length of time pressure is held on the bonded interface were also reported to be important factors influencing hydraulic bonding. Despite, the fundamental contributions of the paper, the testing conditions whether ambient or not were unclarified. For the gas and water test, it was also not clarified if the gas tests were carried out on dry samples or cement samples completely cured with water. Parcevaux and Sault (1984), expanded on the earlier works of Carter and Evans (1964 They eliminated experimental artifacts by designing a setup that allows for both curing and testing of both neat cement systems and those with bonding agents under undisturbed temperature and pressure conditions. However, there were differences between the sample size and type used in their experiments. They reported that hydraulic sealability was a function of the bonding agent and that the hydraulic sealing potential of cement systems was closely linked to its elasticity.

Different test temperatures, pressure, duration, casing, and fluid type have been used for hydraulic testing across the literature. Kamali et al. (2022) carried out both hydraulic and shear bond strength tests with clean and rusty steel pipes. The same cementitious materials used in this study were tested at room temperature with water as a test fluid. The results indicated that there was no correlation between the shear and hydraulic bond strength of the materials and that tortuosity of the rusty pipe surface promotes a higher hydraulic bond strength. Opedal et al. (2018) investigated the sealability of dry and wet-cured cement plugs cured under temperature and pressure. An important conclusion from their findings was that wet-cured samples have higher breakthrough pressures. The hydraulic sealability of cement systems has been validated at small and large-scale (Meng et al., 2021a; Nagelhout et al., 2010; Opedal et al., 2018; Roijmans et al., 2023). Opedal et al. (2018) performed hydraulic sealability tests on cement plugs with two different lengths and different amounts of access to water. They reported that despite having the same breakthrough pressure, the shorter cement plugs exhibit higher flow rates when subjected to the same differential pressure. Nagelhout et al. (2010) introduced laboratory methods for testing out both small and large-scale cement integrity. The small-scale tests were carried out under ambient conditions while the large-scale tests were carried out under temperature and pressure. There was also no consideration for reconciling the differences in mixing energy when preparing the different volumes of slurries required for the large- and small-scale tests. Although the test conditions of the large- and small-scale tests are not the same, they reported a sealability almost 6 times less in the large-scale test than that predicted from the small-scale test. In their findings, they reported a strong effect of the experimental scale on the sealability of the tested cement systems. The foregoing literature discussions show that the hydraulic sealability of cementitious materials can be influenced by their curing and testing conditions. Test temperature, pressure, fluid, casing type, slurry mixing, and duration are some of the factors that can influence the sealing potential of cementitious materials. It is therefore important to develop consistent standard testing procedures which allow for the comparison of the hydraulic sealability of these cementitious materials under representative downhole pressure and temperature.

1.1. *In this study, we aim to examine the following*

- Investigate and report the hydraulic sealability of geopolymers, which are a relatively new alternative to cement, and compare them to conventional API class G cement and current industry standard expansive cement under temperature and pressure conditions.
- Evaluate the influence of the test fluid type on the sealing of the cementitious materials by using nitrogen and water as test fluids.
- Examine the hypothesis of the linear relationship between cement plug length and its hydraulic sealability, on a laboratory scale.

Besides studying the hydraulic integrity of the cementitious plugs,

the findings of this research work reveal the need for a standard for the laboratory testing cement systems and influencing factors to be considered.

1.2. Materials and methods

The experimental procedure in this study is split into two parts: First, the influence of fluid type was examined with the shortest length. Thereafter, a single test fluid was selected and used in the other length test. Fig. 2 shows an infographic for the experimental plan. The following sections present details on the slurry preparation, experimental set-up, and procedure.

1.3. Materials and slurry preparation

Three cementitious materials were used in this experiment. Commercial industrial expansive cement used for plugging and abandonment operations, granite-based geopolymer, and API class G cement were prepared as cement plug-in casing. The API Neat class G cement was as a non-commercial reference for the performance of the other cementitious materials. The mechanical properties of the selected cementitious materials have been recently published (Ogienagbon and Khalifeh, 2022). All the cementitious materials used were mixed using the raw materials and mixing procedure provided by the suppliers. An image of the cementitious materials is presented in Fig. 3 and the detailed recipe for the cementitious materials is provided below.

Neat class G cement - Neat API class G cement manufactured by Dyckerhoff was used to prepare the slurry. The slurry was prepared using deionized water with a water-cement ratio of 0.44.

Geopolymer - The solid phase precursor was dry-blended and mixed according to the recommended in-house recipe. Active quenched blast furnace slag (BFS) was added to naturally occurring aluminosilicate-rich rock to produce a normalized composition. A potassium silicate solution with a modular ratio of 2.49 was used as a hardener. The solid phase

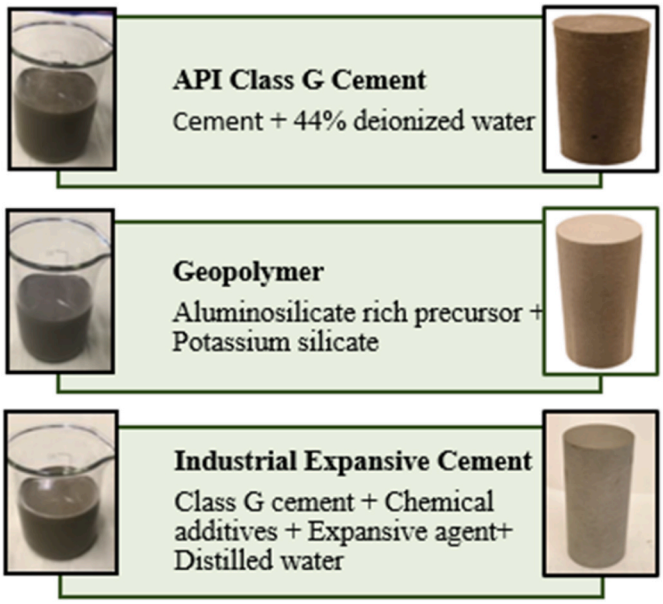

Fig. 3. The cementitious materials in the slurry form (left), and solid form after curing (right). (image is adapted from.

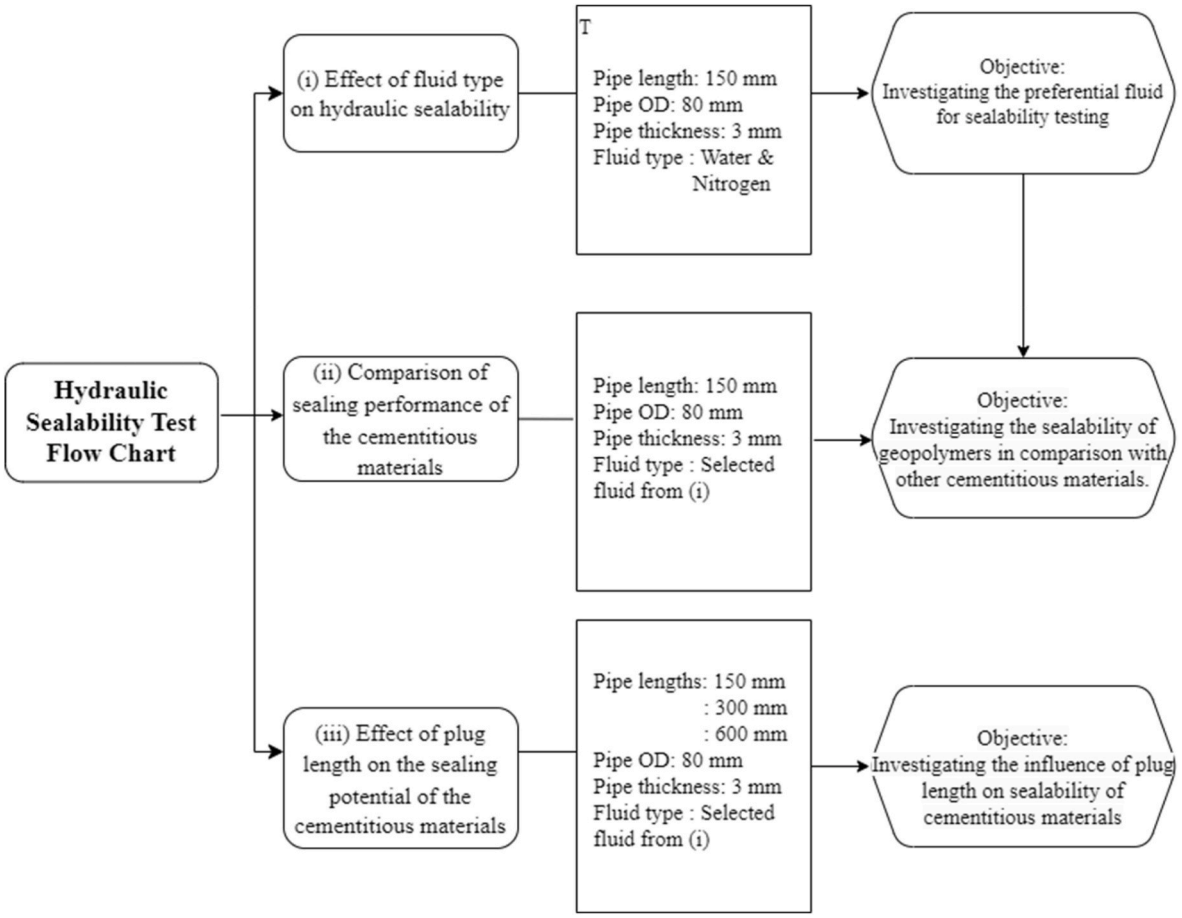

Fig. 2. Infographic of the experimental plan of the study.

precursor was mixed into the liquid potassium silicate solution.

Industrial expansive cement - The material supplier provided both solid phase and industrial additives used in the slurry. The solid phase is composed of class G cement enriched with magnesium oxide as an expansive agent. The industrial chemicals were added to de-ionized water and formed the liquid phase. The industrial additives were used to tailor the rheological and mechanical properties of the slurry. The additives include a retarder, fluid-loss controller, defoamer, cement particle dispersant, and microsilica. The exact proportions of the raw materials are presented in Table 1.

The small-scale slurries were prepared following the API-specified procedure (API RP 10B-2, 2013) with the waring high-speed blender. While a Hobert mixer was used to prepare slurry volumes of 1.5 L and 3.1 L for the medium and large-scale tests respectively. The slurry was mixed at a speed of 281 rpm for 30 min. The mixing time was increased to compensate for the lower mixing speed of the Hobert mixer. After the preparation, the slurries were poured into the casing pipe in the pressure cell and allowed to cure for 7 days at a bottom-hole static temperature (BHST) of 90 °C and 172 bar.

1.4. Experimental methods

Density: The densities of the slurries were measured using the pressurized fluid density balance according to API RP 10B-2 (2013).

Permeability: The bulk permeabilities of the cementitious materials were tested to water using a core flood set-up. A confining pressure of 40 bar was placed around the core to prevent flow through the core-sleeve interface. Constant flow rates were applied on the inlet while the flow on the outlet was monitored, and pressure was allowed to stabilize and recorded. The permeability of the bulk samples was then interpreted using the Darcy law.

Compressive Strength: To measure the compressive strength of the cementitious materials, cement slurries of the same composition as that used in the hydraulic sealability tests were cured with access to water in cylindrical molds. The samples were cured at 90 °C and 172 bar for 7 days. After the curing, the ends of the samples were cut and ground to ensure a smooth and flat surface, and the dimensions were made to maintain length $\geq$2 diameter specifications. Samples were then loaded into the test equipment which was an MTS Criterion C45.105 Load frame. The test was performed in accordance with the recommendations of API RP 10B-2 (2013) with a loading rate of 30 kN/min.

Linear Expansion: The expansion of the geopolymer was evaluated using the annular ring test procedure stated by Recommended Practice on Determination of Shrinkage and Expansion of Well Cement Formulation at Atmospheric Pressure (RP, 2015). The test was carried out for 7 days at ambient conditions. An in-depth discussion of the methodology is presented by Gomado et al. (2023). The expansion results reported for class G were adopted from the experimental works of Gomado et al. (2023) under ambient conditions. The tests were while that of the expansive cement is assumed from widely reported literature (Brooks, 2014). The summary of results and other fluid properties are presented in Table 2.

Table 1
Mix proportions of the cementitious materials used in the study.

		Cementitious Material		
		Neat Class G	Geopolymer	Expansive Cement
Solid Phase **(g)**	Class G cement	700		700
	Aluminosilicate rich rock		350	
	BFS		320	
	Micro Silica		30	
Liquid phase **(By weight % of solid)**	Deionized water	44		33
	Potassium silicate (Modular ratio: 2.49)		44.5	
	Fluid-loss controller			2.8
	Micro silica solution (50%)			11
Chemical Additives **(By weight % of solid)**	Cement dispersant			0.5
	Defoamer			0.1
	Cement retarder			0.6

1.5. Experimental system

The pressure cell and experimental system used to test the hydraulic sealability are presented in Fig. 4. This pressure cell was built in-house and can allow continuous curing and testing of the hydraulic sealability of the specimen. The pressure cell consists of a casing pipe, two end caps and steel metal rods used to fasten the cell together. The steel rods had a diameter of 10 mm and lengths of 220, 360 and 660 mm for the various sample lengths. Both top and bottom endcaps are fitted with access ports that can serve as either injection inlet or production outlet. The top-end cap is equipped with a larger access port that allows the placing of the slurry in the casing pipe. Before placing the slurry in the casing pipe, the bottom endcap is first isolated and silicon grease and filter paper is applied to the bottom end cap to ensure that the cement does not plug into the inlet. The experimental system consists of several tubing, valves, measurement, and data-logging devices used to supply, measure, and log the flow response of water/nitrogen to pressure. The tubings are PFTE with an ID of 0.125 mm, they are inert and can withstand up to 250 °C and pressure rating of 220 bar. The valves were plug valves, and the flow of water was monitored and monitored by the pump and recorded on the computer. The flow meters were mass flow meters with an accuracy of $\pm$0.1% of full scale. Three flow meters connected in parallel with flow range from 0.5 ml/min to 2.5 L/min. An electric oven is used to provide heating for the specimen. The oven covers a temperature range of 20–300 °C. At 90 °C, the oven has a stability of 0.1. A hydraulic pump is used to pressurize the specimen with water during curing and also inject water during the water test. For the gas tests, a nitrogen gas cylinder was connected to a pressure regulator and used to pressurize the specimen. The outlet of the pressure cell at the top is connected to a phase separator which separates produced nitrogen from water and allows the flow rate of water or nitrogen to be measured independently. It should be noted that all the gas measurements reported in the study represent produced gas measurements. Physical confirmation of gas leaks during the gas tests was permitted by observing gas bubbles through the phase separator. For the water test, the flow of water through the specimen was monitored by the three parameters: the injected flow rate, the cumulative volume of water recorded by the pump and the volume of water produced. Conversely, in the gas test, the gas flow rate is measured by the gas flow meter connected to the phase separator. For all the tests the samples were pressurized from the bottom of the cell. In the samples where hydraulic sealability was lost, the permeability and microannuli aperture of the samples were calculated and presented. The casing pipe used in this study has an OD of 80 mm and a thickness of 3 mm. While the pipe diameter and thickness were kept constant, three cement plug lengths of

Table 2
Fluid and Solid properties of the cementitious materials.

	Density (SG)	Bulk Permeability (mD)	Compressive Strength (MPa) @ 7 days	Linear Expansion (%)$^{\Psi}$
API class G	1.90	0.002	40.00	0.022[a]
Geopolymer	1.95	0.003	12.69	0.21
Expansive cement	1.95	0.0003	44.79	1[a]

[a] Adopted from literature ψ Reported at day 7 of curing at ambient temperature and pressure conditions.

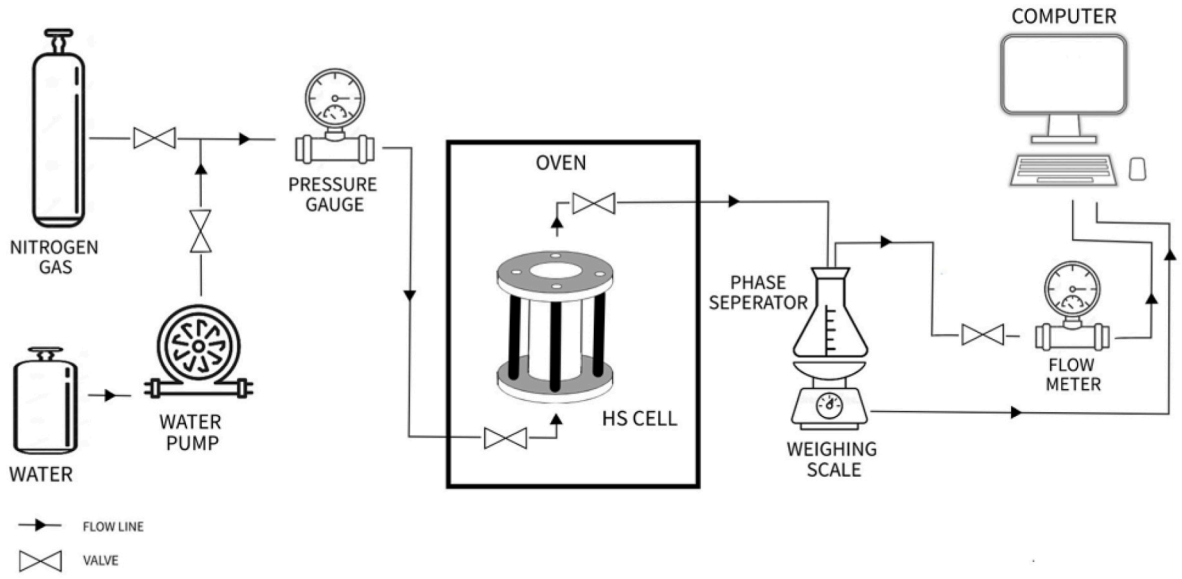

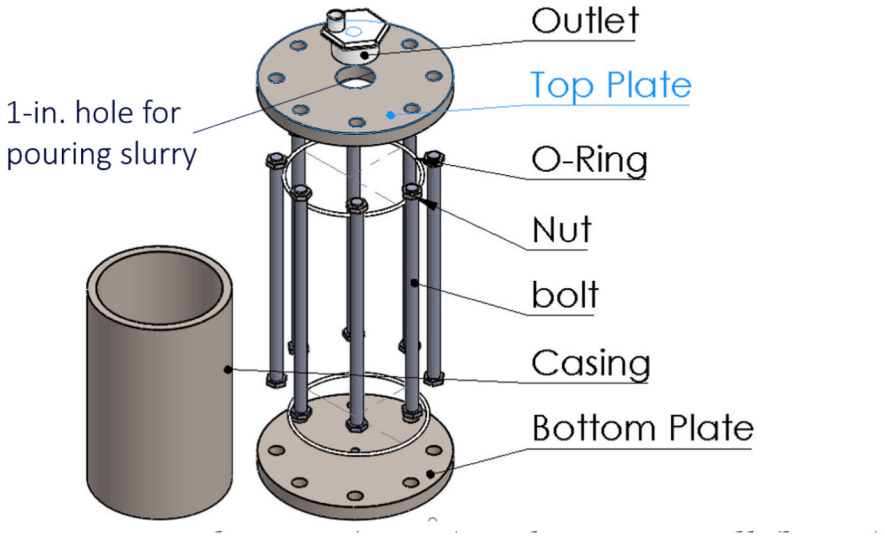

Fig. 4. Experimental set-up (upper) and pressure cell (lower).

150, 300 and 600 mm were evaluated. The mechanical properties of the pipe used in this study are presented in Table 3. The effect of casing ballooning on this casing is calculated according to the radial displacement equation for a closed cylinder presented in Eqn. (1).

$$U_{closed\ end} = \frac{P_1 a}{E\left(b^2 - a^2\right)}\left[(1-2v)a^2 + (1+v)b^2\right] \quad (1)$$

where u represents the radial displacement of the inner cylinder wall in m, a is the inner radius of the cylinder in m, b is the outer radius in m, $P_1 is$ the pressure inside the cylinder, E is Young's modulus in GPa and ν is Poisson's ratio.

Table 3
Casing pipe properties.

Casing Characteristic	Small	Medium	Long
OD (mm)	80		
Thickness (mm)	3		
Young's modulus (GPa)	207		
Poisson's ratio	0.30		
Length (mm)	150	300	600

1.6. Experimental procedure

The hydraulic sealability test was carried out in the following steps.

1. Place the cement slurry into the casing, add a small layer of around 5 mm of de-ionized water and close the cell.
2. Place the pressure cell in the preheated oven at 90 °C and then pressurize the cell with water (from the top) to the curing pressure of 172 bar.
3. Check for any leakages in the system and allow the cement to cure for 7 days under constant pressure.
4. After the curing period, slowly de-pressurize the pressure cell to ambient pressure and then begin pressurizing the cell in steps with water. The pressure is supplied at the bottom of the cell and the flow is monitored at the top of the cell. Each pressure step is held for 30 min according to the NORSOK D010 test recommendation (NORSOK D-010, 2021).

5. Decrease the pressure slowly to ambient conditions and then repeat the procedure using gas.
6. Estimate the permeability and microannulus aperture created by both fluids.

The effective permeability of the casing-cement interface to water and gas can be interpreted using Darcy's law for incompressible and compressible fluids presented through Eqns. (2) and (3). The measured flow rates and differential pressures are also related to the effective microannulus (Aas et al., 2016; Stormont et al., 2018) created by water and gas using Eqns. (4) and (5).

$$Q = \frac{KA\,(P_u - P_d)}{\mu L} \tag{2}$$

$$Q_g = \frac{K_g M\left(P_u^2 - P_d^2\right)A}{2\mu z R_c T L} \tag{3}$$

$$Q = \frac{Wh^3(P_u - P_d)}{12\mu L} \tag{4}$$

$$Q_g = \frac{Wh^3\left(P_u^2 - P_d^2\right)}{24\mu R T L \rho_d} \tag{5}$$

Although the units of measurements are measured in field units, the values were converted to SI units during calculations. Where P_u and P_d represents upstream and downstream pressure at the inlet and outlet measured in bar and interpreted in Pa respectively; K is the permeability of the fluid in mD the subscript g refers to the gas properties; A is the area in m; Z is the compressibility factor; Q is the flow rate measured in ml/min and interpreted in m^3/sec. W is the circumference of the inner wall of the pipe in m; ρ is the gas density at downstream in kg/m^3; T is temperature in measured in C and interpreted in K; L is the length of the plug in m; μ is fluid viscosity measured in cp and interpreted in Pa.s; while R represents the specific gas constant for nitrogen in J/kg*K; R_c is the gas constant in J mol^{-1} K^{-1}; M is the molar mass of nitrogen in kg/mol.

2. Results and discussion

2.1. Effect of fluid type on hydraulic sealability

The measurement of the sealing performance of cementitious materials requires the pressurization of the casing pipe at various pressures. This can lead to ballooning of the casing especially at high pressures. Casing ballooning mimics a worst-case scenario and can lead to an underestimation of the sealing performance of the cementitious material. One of the main objectives of this study is to examine the individual sealing performance of the cementitious materials owing to the chemistry of the material itself therefore, it is important to estimate and account for microannuli caused due to ballooning. During curing, the estimated radial deformation at the curing pressure is 35.18 μm according to Fig. 5. This implies that the slurry cures and takes the shape of the radially ballooned casing. At the start of the test, the sample is depressurized to ambient pressure, causing the casing to return to its initial dimensions. This retraction may cause a false sealing of the casing on the plug. It should be noted that this phenomenon represents a conservative test condition. However, since this occurs consistently through the samples, the results between the cementitious materials remain comparable. The permeability of the cementitious materials used in this study has been reported to be ultra-low (Khalifeh et al., 2019; Stormont et al., 2015). The bulk permeability of the API class G, geopolymer and expansive cement used in this study was measured by core-flooding with water. A permeability of 0.002, 0.003 and 0.0003 mD was obtained for class G, geopolymer and expansive cement, respectively. The permeability of both materials is orders of magnitude lower than that of a typical leaking specimen. Due to the ultra-low

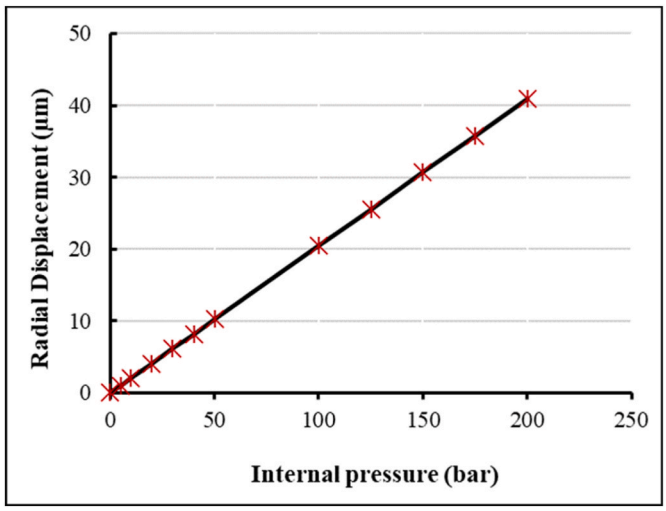

Fig. 5. Effect of casing internal pressure on the radial displacement – the red dots represent the measurement points.

permeabilities measured, the matrix permeabilities of the cementitious materials were then considered to be insignificant and flow was assumed to occur predominantly through the microannuli at the cement plug-casing interface. A minimum of three parallel tests were done for each cementitious material. This was done to test the reproducibility of the experiments. For clarification, the term breakthrough pressure used across the study refers to the pressure required to create communication of flow through the microannulus. The hydraulic sealability of one of the expansive cement samples, EXP 1, was tested with both water and gas. Fig. 6 presents the results for both the water and gas test. The blue line represents the differential pressure in bars while the red line represents the flow rate through the cement plug sample in ml/min. The sharp peaks in flow rate seen in the graph for the water test should not be confused with a breakthrough of fluid, but rather the response of the pump to meet set pressure. For each pressure step, the pressure was held for 30 min, this duration was selected to allow the completion of a test within a day-hour work period. During the water test shown in Fig. 6a, no flow was detected up to a 10 bar pressure differential, at which a seeping flow rate of about 0.003 ml/min is recorded. At the maximum pressure differential of 30 bar, a maximum flow rate of 0.04 ml/min is recorded. After the completion of the water test, gas was injected. Upon injecting gas into EXP 1, its gas-sealability was lost around 10 bar which is the same breakthrough pressure recorded during the water test. A subsequent increase in pressure is also followed by an increase in flow rate for both fluids. The measurements show that the test fluid type did not influence the breakthrough pressure. In fact, it appears that the microannuli formed at the casing-cement interface during the water test reseals itself when the sample is de-pressurized and that a minimum pressure of 10-bar is required to reopen the microannuli again during the gas test. Fig. 7 shows the relationship between differential pressure with flow rate and microannuli aperture for the water tests. The Figure shows good repeatability amongst the test samples. Expansive cement generally required a minimum differential pressure of around 10–15 bar before flow is initiated.

The samples were also characterized by very low flow rates throughout the test. This suggests that there is good bonding at the cement-casing interface and that the expansive cement does not fail catastrophically when the integrity is compromised. The microannuli aperture of the test samples was found to generally grow with increasing pressure until around 25 bar. After 25 bar, further pressure increases had little effect on the microannuli aperture. We assume that the terminal microannuli aperture is reached at this pressure and that a single phase, laminar flow is achieved. A similar response of increasing microannuli aperture with pressure is also observed during the gas test shown in

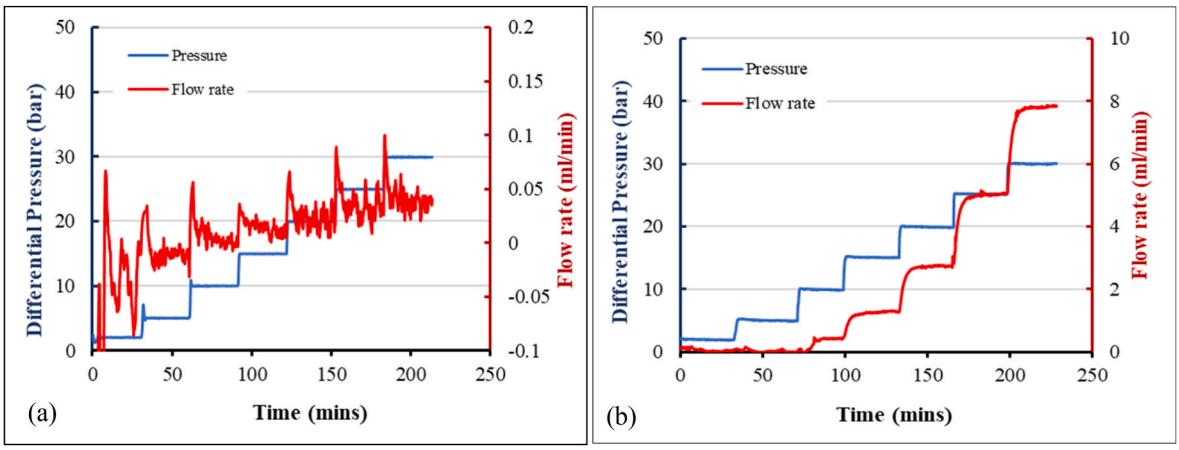

Fig. 6. Hydraulic sealability of expansive cement to water (a) and gas (b).

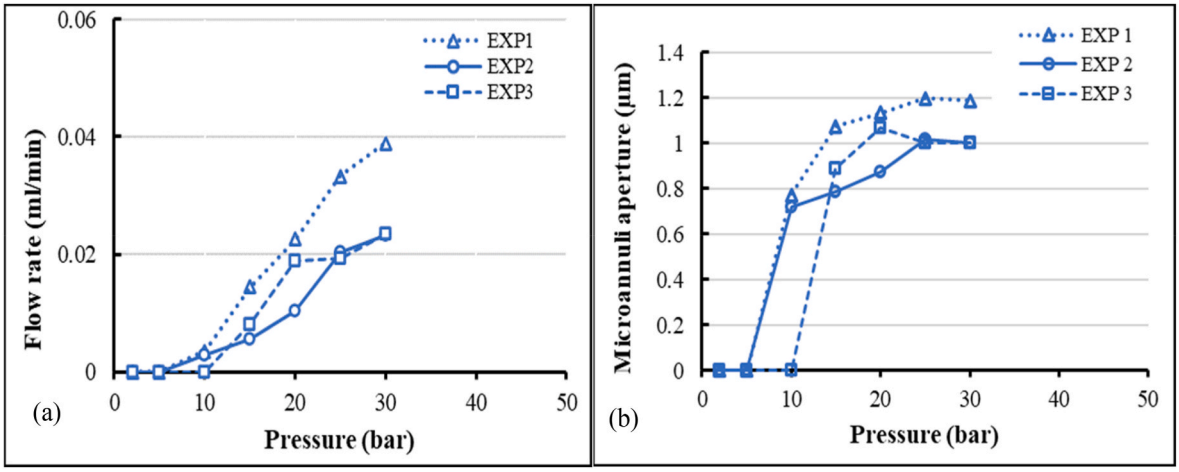

Fig. 7. (a) Relationship between applied differential pressure and flow rate, (b) Relationship between applied differential pressure and microannuli aperture for the water tests.

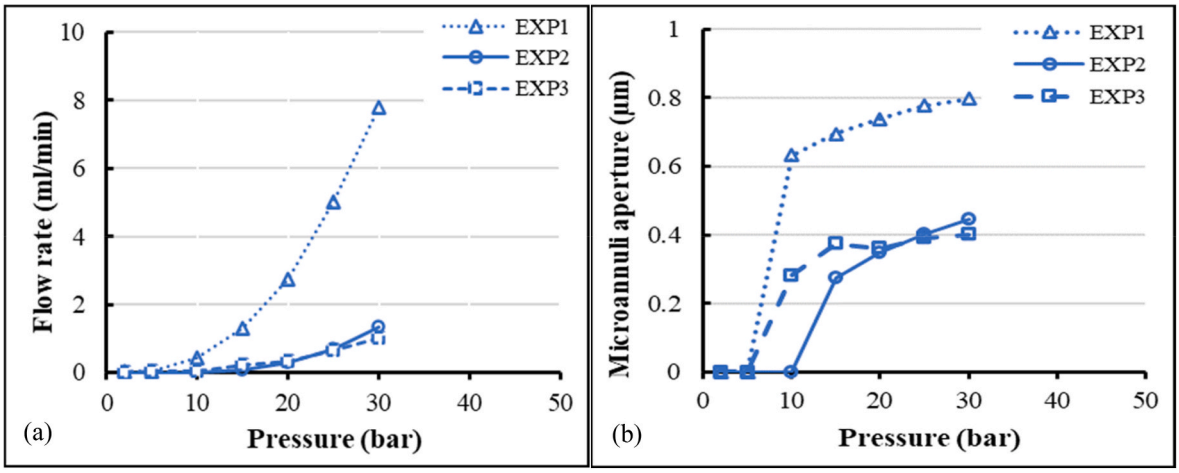

Fig. 8. (a) Relationship between applied differential pressure and flow rate, (b) Relationship between applied differential pressure and microannuli aperture for the gas tests.

Fig. 8. Eqns. (4) and (5) were used to fit a single microannuli aperture which is valid for the measured sets of pressure and flow rates for both water and gas tests presented in Figs. 7 and 8 and presented in Table 4.

It should be noted that the microannuli aperture values reported in the study are based on the cubic law, which assumes that the microannuli is constant and uniformly distributed along the cement plug-casing interface. This is a simplification of the true behaviour of microannuli which has been reported to be non-smooth and randomly

Table 4
Summary of results.

Sample	Expansive Cement					
	Water			Gas		
	Breakthrough Pressure (bar)	K (mD)	h (μm)	Breakthrough Pressure (bar)	K (mD)	h (μm)
EXP 1	10	0.01	1.32	10	0.0025	0.81
EXP 2	10	0.007	1.13	15	0.00050	0.48
EXP 3	15	0.005	1.06	10	0.00031	0.41

distributed along the cement-casing interface (Ogienagbon et al., 2021). The microannuli apertures presented in Table 4 are based on the modelled values. Although the fluid type used as test fluid did not considerably affect the breakthrough pressure, the magnitude of water and gas permeabilities differ by an order of 1. The reported lower gas permeability compared to water is consistent with the findings of Meng et al. (2021b). This lower permeability of gas is suspected to be due to the lower viscosity of nitrogen and also the two-phase flow system occurring in the microannulus. During the water test, water is injected into a microannuli aperture fully saturated with water, however, during the gas test, gas is injected into a microannuli fully saturated with water. Gas flow will primarily occur through the large flow paths, bypassing smaller water-filled flow paths with higher capillary pressure along the plug-casing interface. The gas permeability, in this case, cannot be compared to the gas permeability of a completely dry microannuli where there is a single-phase flow. The lower gas sealability reported by Carter and Evans (1964) is suspected to be due to the testing being done on dry cured samples. Both the estimated and modelled microannuli aperture for gas was also considerably smaller than for water, this is no surprise based on the foregoing discussion since $K \sim h^3$. It is also assumed that no casing ballooning occurred during testing since assuming ballooning was to occur during the testing, the estimated radial deformation at the differential pressure of 30 bar would be 6.14 μm which is much less than the modelled and estimated aperture of both fluids. When comparing the performance of both fluids, gas leaks through the small-sized microannuli apertures at the casing-cement interface were easier detected compared to water leaks. However, the estimated microannuli apertures from the water test are more realistic. We propose that gas tests be considered if the main objective of a test is to test the sealing performance of a cement system. When the focus of a test is to estimate the microannuli aperture, then water is suggested as a preferential test fluid.

2.2. Sealing performance of the cementitious materials

The hydraulic sealability of the three cementitious materials was tested at a small scale with gas as the test fluid. Gas was selected as test fluid due to its easier leak detectability as discussed in the foregoing. The sealing performance of the cementitious materials is presented in Fig. 9. The reference class G cement shows no restriction to flow as seen in Fig. 9a. The smallest differential pressure applied, 2 bar was enough to initiate flow through all the class G test duplicates. This implies that the flow restriction of class G cement was poor. The class G samples also experience higher flow rates under the same differential pressure than the other cementitious materials. This implies that the reference G cement is more susceptible to autogenous shrinkage during curing which prevents it from providing adequate bonding to the casing pipe. This is consistent with our expectations as neat G cement has been reported to only have a linear expansion of 0.022% (Gomado et al., 2023). The autogenous shrinkage faced by Neat G cement has also been previously discussed extensively by previous researchers (Khalifeh et al., 2018a: Sasaki et al., 2018; Shen et al., 2015). For expansive cement presented in Fig. 9b, the effect of the expansive agent in the slurry is apparent in its resistance to flow until around 10–15 bar. Upon the loss of sealability in the expansive cement system, the increase in measured flow due to increased pressure did not grow exponentially like that of class G. This demonstrates that expansive cement does not fail catastrophically but only permits gas to seep through the microannuli. The relationship between the differential pressure and measured flow rates for geopolymer is presented in Fig. 9c. Only two samples were tested in this case due to pressure loss on the third sample during curing. Upon testing of the geopolymer systems, no leak was detected up to the maximum test pressure of 30 bar. This result infers that geopolymers have sufficient expansion to promote good bonding with the pipe thereby mitigating leaks at the cement plug-pipe interface. The results also show that geopolymers have good sealing potential at high temperature. The hydraulic sealing potential of cementitious material have been linked to its elasticity (Parcevaux and Sault, 1984). Cement with high elasticity was observed to have higher sealing potential. Geopolymers have been reported to be capable of maintaining high elasticity under low temperature and high temperature (Ogienagbon and Khalifeh, 2022) which can then promote its hydraulic sealability. The high hydraulic sealing potential of geopolymers observed in this study further validates the findings of Kamali et al. (2022) which investigated the sealing potential of geopolymers at ambient temperature and reported the superior hydraulic sealing potential of geopolymers compared to the other cementitious materials.

2.3. Effect of plug length on the sealing potential of the cementitious materials

The development of any cementitious material requires small-scale

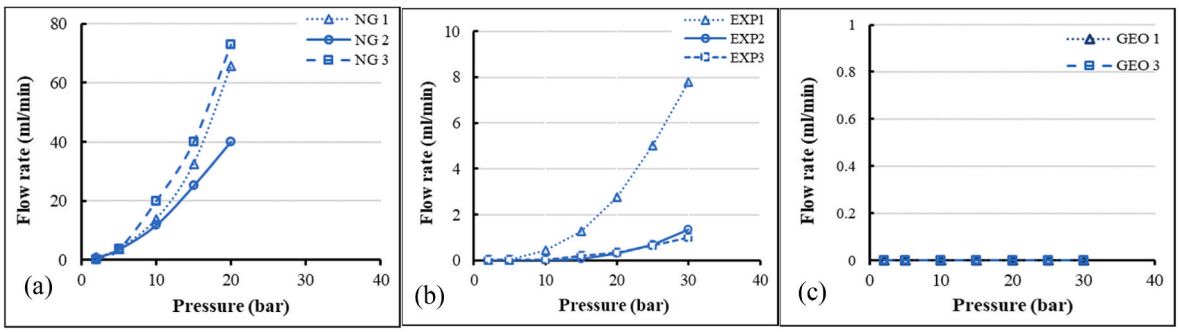

Fig. 9. Hydraulic sealing results for the cementitious materials (NG represents neat G cement, EXP represents expansive cement, GEO represents geopolymer).

laboratory testing, which then is adapted to large-scale and eventual field case implementation. It is quite pertinent to be able to predict the performance of large-scale tests from small-scale tests. We compare the sealing performance of the three cementitious materials with a constant diameter over three lengths and present the results in Fig. 10a–i. Fig. 10a–c presents the effect of plug length on the sealing potential of Neat G cement, Fig. 10d–f shows that of geopolymers, and Fig. 10g–i represents that of expansive cement. When conducting the tests, efforts were made to eliminate operational factors, which may influence the performance of the materials like mixing energy (Saleh et al., 2019), pipe roughness (Corina et al., 2020), or pipe chemical composition (Khalifeh et al., 2018a). Due to the length scale, the smallest plugs were subjected to the highest gradient, while the longest plug samples generally experienced a longer pressure differential across their length. For the smallest plug length, the minimum pressure gradient applied is 13.3 bar/m, for the medium plug length, it is 6.7 bar/m, and the minimum pressure gradient of the longest plug length is 3.3 bar/m. The results do not show a clear trend and the effect of increasing the plug length appears to be unsystematic in all the three cementitious materials tested. There also seems to be distinctively poorer sealing in the medium-length class G and geopolymer plugs. This is a clear violation of the Darcy law. According to Darcy's law, given that all other variables are constant, a two-time increase in length should cause a reduction in flow rate by half. Applying this theory to our results would give the hypothesis of a linear relationship between the cement plug length and its hydraulic sealability. This should imply that the small-scale experiments should give the worst sealing, while the longest plugs should give the best sealing. This was consistent with the model findings of Al Ramadan et al. (2019), who concluded that longer cement plugs give better sealing. Conversely, dissenting views were expressed from the experimental findings of Nagelhout et al. (2010) where they reported that small-scale experiments provided better sealing than the large-scale test. However, in their experiments, the small and large-scale experiments differ in diameter and length. These peculiar results indicate that there are several other factors that can influence the curing of cementitious materials. It is suspected that the slurry volume plays a major role in how the cementitious material cures, thereby influencing its shrinkage and bonding with the casing. Slurries of different volumes may also cure slightly differently, this is because the amount of heat generated during the hydration of larger volumes of slurry is higher than

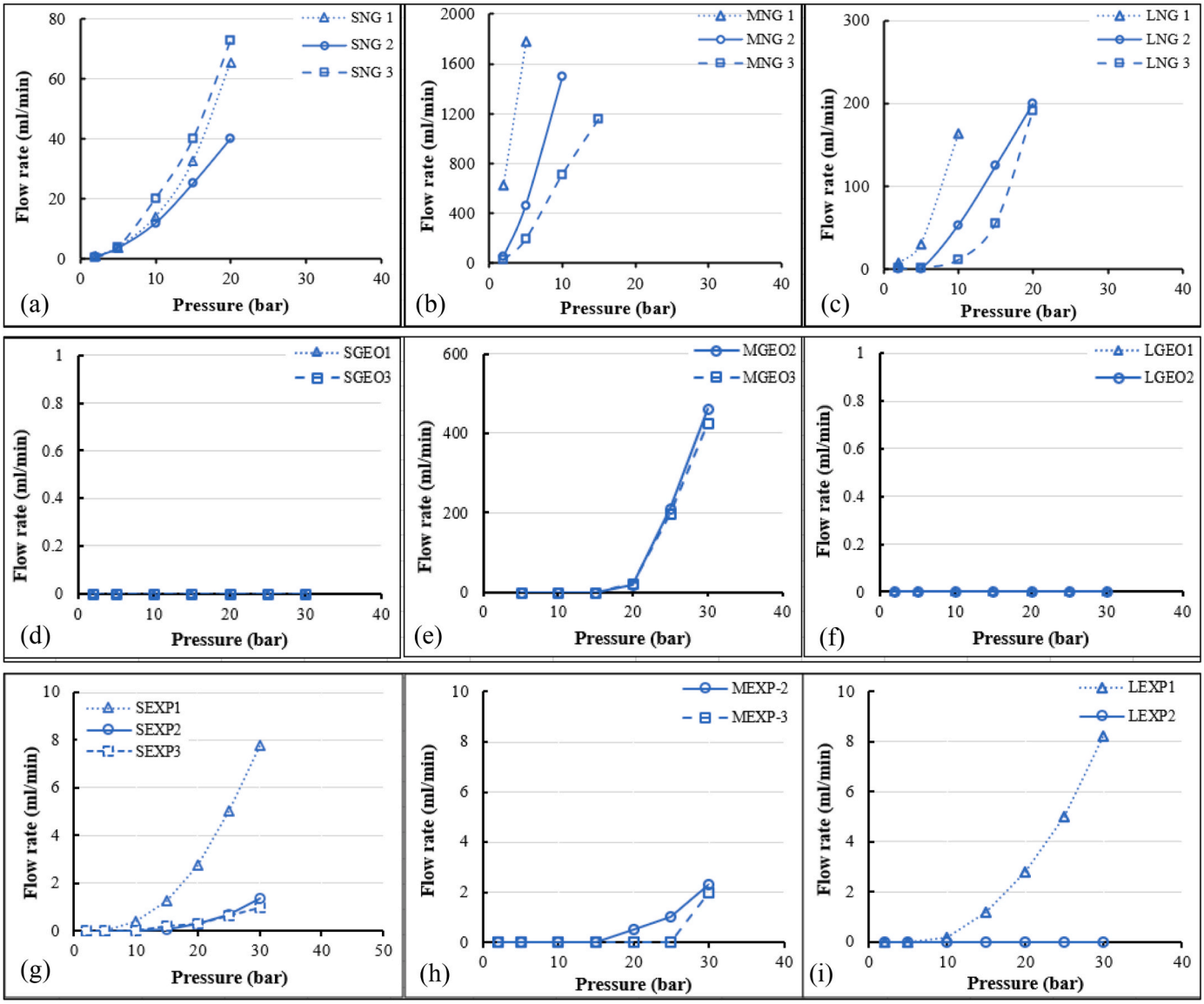

Fig. 10. Effect of cement plug length on its hydraulic sealability; (a–c) represents Neat G, (d–f) represents geopolymer, (g–i) represents expansive cement; The letters S, M, and L represents the small, medium, and long lengths of the cement plugs.

that in smaller volumes (Ravi et al., 2009). There is also a need to point out that temperature influences the hydration kinetics and early-age shrinkage of cementitious materials (Elkhadiri et al., 2009; Lura et al., 2001; Maltais and Marchand, 1997). Although the influence of temperature will also depend on the chemical composition of the slurry, it is generally accepted that higher temperatures may lead to higher stresses and faster shrinkage of the cement which then influences its hydraulic sealability. It has also been reported that there is a negative influence of length on the shear bond of cement when the length-to-diameter ratio exceeds 1.5 (Parcevaux and Sault, 1984). However, it is unclear how this may influence the hydraulic sealability of the cementitious materials as all the test samples in our study have a length-to-diameter ratio higher than 1.5. The results show that the linear relationship between cement plug length and its hydraulic sealability predicted by cement models may not be sufficient to describe real laboratory conditions and there is a need for standardized cement testing methods to encourage repeatability and predictability of cement performance in larger scales.

3. Conclusion

This paper investigated the hydraulic integrity of three cementitious materials: API class G, granite-based geopolymer, and expansive cement. We also compared the impact of the test fluid on the sealing performance of these materials and then investigated the effect of the plug length on sealing performance. Based on the results discussed in the preceding sections, the following conclusions can be drawn.

- Cementitious materials such as granite-based geopolymer and expansive cement demonstrate promising performance as plugs.
- The geopolymer experience expansion during the curing process, enhancing its hydraulic sealability.
- Type of test fluid does not significantly affect the sealing performance of the cementitious materials. The selection of test fluid should be based on the specific objectives and test setup.
- Increasing the length of the cement plug does not linearly improve its sealing performance as predicted by cement models.
- Various factors, such as slurry volume may influence the cement hydration and curing process.

In order to enhance cement testing methods, it is recommended to develop standardized test protocols for hydraulic sealability testing. These generalized test standards would contribute to more reliable and consistent evaluation of the performance of cementitious materials.

Unit Conversion Factors.

Bar = 100,000 Pa.

°C = 273.15 K

ml/min = 1,67 E−8 m^3/sec

mD = 9.86 m^2

Declaration of competing interest

The authors declare the following financial interests/personal relationships which may be considered as potential competing interestsAdijat A. Ogienagbon reports financial support was provided by Research Council of Norway. Adijat A. Ogienagbon reports financial support was provided by NORCE Norwegian Research Centre AS Stavanger. Adijat A. Ogienagbon reports equipment, drugs, or supplies was provided by Halliburton.

Data availability

Data will be made available on request.

Acknowledgements

This work has been funded by the Research Council of Norway (RCN) and NORCE through the project "#308767 - Fluid migration modelling and Treatment project. The authors would like to thank Halliburton for providing some chemicals for use in this project.

References

Aas, B., et al., 2016. Cement placement with tubing left in hole during plug and abandonment operations. IADC/SPE drilling conference and exhibition. OnePetro. https://doi.org/10.2118/178840-MS.

Adjei, S., Elkatatny, S., Aggrey, W.N., Abdelraouf, Y., 2022. Geopolymer as the future oil-well cement: a review. J. Petrol. Sci. Eng. 208, 109485 https://doi.org/10.1016/j.petrol.2021.109485.

Al Ramadan, M., Salehi, S., Teodoriu, C., 2019. Robust Leakage Modeling for Plug and Abandonment Applications, International Conference on Offshore Mechanics and Arctic Engineering. American Society of Mechanical Engineers. https://doi.org/10.1115/OMAE2019-95612. V008T11A054.

API RP 10B-2, 2013. American Petroleum Institute, API: Recommended Practice for Testing Well Cements. API, Washington, DC. API.

Bois, A.-P., Garnier, A., Rodot, F., Saint-Marc, J., Aimard, N., 2011. How to prevent loss of zonal isolation through a comprehensive analysis of microannulus formation. SPE Drill. Complet. 26 (1), 13–31. https://doi.org/10.2118/124719-PA.

Brooks, J., 2014. Concrete and Masonry Movements. Elsevier Science.

Carter, L., Evans, G., 1964. A study of cement-pipe bonding. J. Petrol. Technol. 16 (2), 157–160. https://doi.org/10.2118/764-PA.

Corina, A.N., Opedal, N., Vrålstad, T., Skorpa, R., Sangesland, S., 2020. The effect of casing-pipe roughness on cement-plug integrity. SPE Drill. Complet. 35 (2), 237–251. https://doi.org/10.2118/194158-PA.

Davies, R.J., et al., 2014. Oil and gas wells and their integrity: implications for shale and unconventional resource exploitation. Mar. Petrol. Geol. 56, 239–254. https://doi.org/10.1016/j.marpetgeo.2014.03.001.

Eid, E., Tranggono, H., Khalifeh, M., Salehi, S., Saasen, A., 2021. Impact of drilling fluid contamination on performance of rock-based geopolymers. SPE J. 26 (6), 3626–3633. https://doi.org/10.2118/205477-PA.

Elkhadiri, I., Palacios, M., Puertas, F., 2009. Effect of Curing Temperatura on Hydration Process of Different Cement. Czech Academy of Sciences. http://hdl.handle.net/10261/35190.

Gomado, F.D., Khalifeh, M., Aasen, J.A., 2023. Expandable Geopolymers for Improved Zonal Isolation and Plugging, SPE/IADC International Drilling Conference and Exhibition. https://doi.org/10.2118/212493-MS. OnePetro.

Geiker, M., Knudsen, T., 1982. Chemical shrinkage of Portland cement pastes. Cement Concr. Res. 12 (5), 603–610. https://doi.org/10.1016/0008-8846(82)90021-7.

Kamali, M., Khalifeh, M., Eid, E., Saasen, A., 2022. Experimental study of hydraulic sealability and shear bond strength of cementitious barrier materials. J. Energy Resour. Technol. 144 (2) https://doi.org/10.1115/1.4051269.

Khalifeh, M., Hodne, H., Saasen, A., Dziekonski, M., Brown, C., 2018a. Bond strength between different casing materials and cement, SPE Norway one day seminar. OnePetro. https://doi.org/10.2118/191322-MS.

Khalifeh, M., Hodne, H., Saasen, A., Dziekonski, M., Brown, C., 2018b. Bond Strength between Different Casing Materials and Cement, SPE Norway One Day Seminar. Society of Petroleum Engineers, Bergen, Norway. https://doi.org/10.2118/191322-MS.

Khalifeh, M., Saasen, A., 2020. Introduction to Permanent Plug and Abandonment of Wells. Springer Nature. https://doi.org/10.1007/978-3-030-39970-2.

Khalifeh, M., Saasen, A., Hodne, H., Motra, H.B., 2019. Laboratory evaluation of rock-based geopolymers for zonal isolation and permanent P&A applications. J. Petrol. Sci. Eng. 175, 352–362. https://doi.org/10.1016/j.petrol.2018.12.065.

Lavrov, A., Todorovic, J., Torsæter, M., 2015. Numerical Study of Tensile Thermal Stresses in a Casing-Cement-Rock System with Heterogeneities, 49th US Rock Mechanics/Geomechanics Symposium. OnePetro.

Lura, P., van Breugel, K., Maruyama, I., 2001. Effect of curing temperature and type of cement on early-age shrinkage of high-performance concrete. Cement Concr. Res. 31 (12), 1867–1872. https://doi.org/10.1016/S0008-8846(01)00601-9.

Maltais, Y., Marchand, J., 1997. Influence of curing temperature on cement hydration and mechanical strength development of fly ash mortars. Cement Concr. Res. 27 (7), 1009–1020. https://doi.org/10.1016/S0008-8846(97)00098-7.

Meng, M., et al., 2021a. Predicting cement-sheath integrity with consideration of initial state of stress and thermoporoelastic effects. SPE J. 26 (6), 3505–3528. https://doi.org/10.2118/205344-PA.

Meng, M., Frash, L.P., Chen, B., Welch, N.J., Li, W., Carey, J.W., 2021, June. Experimental study of water and CO2 transport along the casing-cement interface. In: ARMA US Rock Mechanics/Geomechanics Symposium. ARMA, p. ARMA-2021.

Nagelhout, A., et al., 2010. Laboratory and field validation of a sealant system for critical plug-and-abandon situations. SPE Drill. Complet. 25 (3), 314–321. https://doi.org/10.2118/97347-PA.

Norsok D-010, 2021. D-010 Well integrity in drilling and well operations. Standards Norway, Norway.

Ogienagbon, A., Khalifeh, M., 2022. Experimental evaluation of the effect of temperature on the mechanical properties of setting materials for well integrity. SPE J. 1–13 https://doi.org/10.2118/209794-PA.

Ogienagbon, A., Khalifeh, M., Yang, X., Kuru, E., 2021. Manuscript Title: Characterization of Microannuli at the Cement-Casing Interface: Development of Methodology, Abu Dhabi International Petroleum Exhibition & Conference. https://doi.org/10.2118/207581-MS. OnePetro.

Opedal, N., Corina, A.N., Vrålstad, T., 2018. Laboratory Test on Cement Plug Integrity, International Conference on Offshore Mechanics and Arctic Engineering. American Society of Mechanical Engineers. https://doi.org/10.1115/OMAE2018-78347. V008T11A071.

Parcevaux, P., Sault, P., 1984. Cement Shrinkage and Elasticity: a New Approach for a Good Zonal Isolation, SPE Annual Technical Conference and Exhibition. SPE. https://doi.org/10.1115/OMAE2018-78347. SPE-13176-MS.

Ravi, K., Iverson, B., Moore, S., 2009. Cement-slurry design to prevent destabilization of hydrates in deepwater environment. SPE Drill. Complet. 24 (3), 373–377. https://doi.org/10.2118/113631-PA.

Roijmans, R.F., Wolterbeek, T.K., Cornelissen, E.K., Keultjes, W.J., 2023. Quantifying the Sealing Performance of Plug and Abandonment (P&A) Cement Systems under Downhole Conditions. SPE/IADC Drilling Conference and Exhibition. SPE. https://doi.org/10.2118/212542-MS. D031S024R001.

RP, A.S.P., 2015. Recommended Practice on Determination of Shrinkage and Expansion of Well Cement Formulations at Atmospheric Conditions.

Saleh, F.K., Salehi, S., Teodoriu, C., 2019. Experimental investigation of mixing energy of well cements: the gap between laboratory and field mixing. J. Nat. Gas Sci. Eng. 63, 47–57. https://doi.org/10.1016/j.jngse.2019.01.004.

Sasaki, T., Soga, K., Abuhaikal, M., 2018. Water absorption and shrinkage behaviour of early-age cement in wellbore annulus. J. Petrol. Sci. Eng. 169, 205–219. https://doi.org/10.1016/j.petrol.2018.05.065.

Shen, W., et al., 2015. Quantifying CO2 emissions from China's cement industry. Renew. Sustain. Energy Rev. 50, 1004–1012. https://doi.org/10.1016/j.rser.2015.05.031.

Sherir, M.A., Hossain, K.M., Lachemi, M., 2017. Development and recovery of mechanical properties of self-healing cementitious composites with MgO expansive agent. Construct. Build. Mater. 148, 789–810. https://doi.org/10.1016/j.conbuildmat.2017.05.063.

Stormont, J., Ahmad, R., Ellison, J., Reda Taha, M., Matteo, E., 2015. Laboratory Measurements of Flow through Wellbore Cement-Casing Microannuli, 49th US Rock Mechanics/Geomechanics Symposium. OnePetro.

Stormont, J.C., Fernandez, S.G., Taha, M.R., Matteo, E.N., 2018. Gas flow through cement-casing microannuli under varying stress conditions. Geomechanics for Energy and the Environment 13, 1–13. https://doi.org/10.1016/j.gete.2017.12.001.

van Eijden, J., Cornelissen, E., Ruckert, F., Wolterbeek, T., 2017. Development of Experimental Equipment and Procedures to Evaluate Zonal Isolation and Well Abandonment Materials, SPE/IADC Drilling Conference and Exhibition. https://doi.org/10.2118/184640-MS. OnePetro.

Watson, T.L., Bachu, S., 2009. Evaluation of the potential for gas and CO2 leakage along wellbores. SPE Drill. Complet. 24 (1), 115–126. https://doi.org/10.2118/106817-PA.